Dalton Transactions

Accepted Manuscript

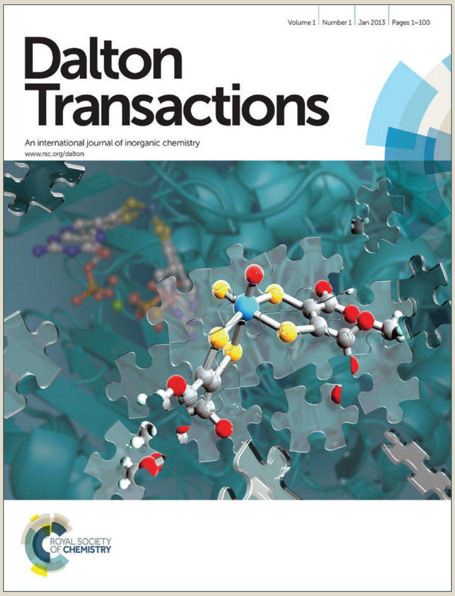

www.rsc.org/dalton

Cite this: DOI: 10.1039/c0xx00000x

www.rsc.org/xxxxxx

ARTICLE TYPE

Highly soluble gadofullerene salt and its magnetic property †

Yongqiang Feng[‡a], Jie Li[‡a], Zhuxia Zhang[b], Bo Wu[a], Yongjian Li[a], Li Jiang[a], Chunru Wang[a], and Taishan Wang*[a]

Received (in XXX, XXX) Xth XXXXXXXXX 20XX, Accepted Xth XXXXXXXXX 20XX
DOI: 10.1039/b000000x

A kind of Gd@C_{82} salt, Gd@C_{82}/TBPA, was prepared through chemical oxidation. The Gd@C_{82}/TBPA was characterized to be paramagnetic with effective magnetic moment of 9.68 μ_B. The Gd@C_{82}/TBPA can dissolve in many organic solvents and such high solubility will make it more applicable as magnetic material.

Gadolinium endohedral metallofullerenes (gadofullerenes) are of particular importance because of their high electron spin from the half-filled 4*f* electronic shell of internal Gd^{3+} ion with orbital angular momentum of 7/2,[1-11] making them to serve as outstanding magnetic resonance imaging (MRI) contrast agents.[12-19] Gadofullerenes offer the stable entrapment of otherwise toxic Gd^{3+} ions and the rich exterior functionalization on outer fullerene cages. The Gd@C_{2v}-C_{82} (referred as Gd@C_{82} for clarity) is a typical case for gadofullerenes,[8-11] whose water-soluble derivatives have been extensively studied as MRI contrast agents and antitumor medicine.[12-15,20-22] However, more applications of Gd@C_{82} are limited to its serious agglomeration and poor solubility in solvents. Therefore, it is essential to modify the Gd@C_{82} and to make it highly soluble without distorting its structure and magnetic property.

For gadofullerenes, the effective magnetic moment (μ_{eff}) is often calculated to evaluate their magnetic property.[23-29] The μ_{eff} is related to many physical parameters, such as proton relaxation rate of MRI contrast agents,[17] electron spin orientation,[30] dipole-dipole interactions,[31] etc. For gadofullerenes, the reported μ_{eff} of the widely studied Gd@C_{82} was 6.9 μ_B (μ_B is Bohr magneton).[29] However, the μ_{eff} value of Gd@C_{82} is smaller than that of one free Gd^{3+} (7.94 μ_B).[29] Such reduced μ_{eff} in Gd@C_{82} has been expected to be mainly caused by the antiferromagnetic coupling interaction of the spin (S = 1/2) on the π orbitals of the fullerene cage and the octet spin (S = 7/2) of the encapsulated Gd^{3+} ion.[26-29] To resolve these problems, one method is to wipe out the unpaired spins on the C_{82} cage of Gd@C_{82}, in order to cut off the generic antiferromagnetic coupling between the 4*f* electrons and cage-based unpaired spin.

Herein, we synthesized a kind of Gd@C_{82} salt, Gd@C_{82}/TBPA, whose μ_{eff} is enhanced due to the eliminated unpaired spin on C_{82} cage and antiferromagnetic coupling. Unprecedentedly, the as-prepared Gd@C_{82}/TBPA has excellent solubility and it can dissolve in many organic solvents. Such high solubility will make it more applicable as magnetic materials.

Figure 1a shows the structure of Gd@C_{82}, which has a C_{2v}-C_{82} cage and an encapsulated Gd^{3+},[8-10] synthesized by arc-discharging method and characterized by high performance liquid chromatography (HPLC) and matrix-assisted laser desorption/ionization time of flight mass spectrometry (MALDI-TOF-MS) (Figure S1-S4). The tris(4-bromophenyl)ammonium hexachloroantimonate ($(p\text{-}BrC_6H_4)_3N^+SbCl_6^-$, TBPA), as shown in Figure 1a, is a suitable oxidant as can be seen from the redox potentials shown in Table S1.[32]

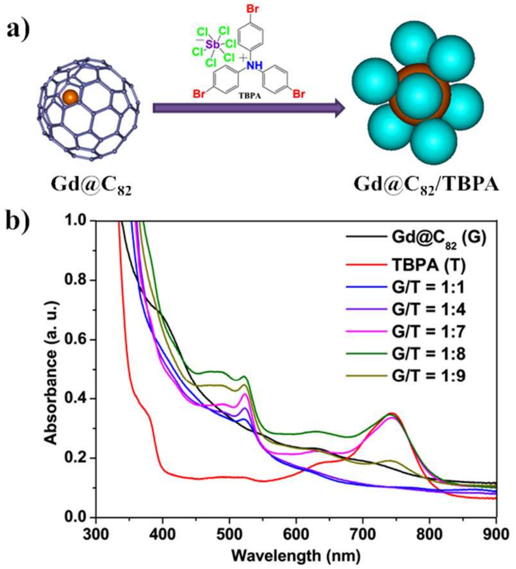

Figure 1. a) Structures of Gd@C_{82}, TBPA and their complex Gd@C_{82}/TBPA. b) The UV-Vis-NIR spectra of Gd@C_{82} (G) and TBPA (T) mixture with varied molar ratios in ODCB solution.

The oxidation process was performed by addition of TBPA into the *o*-dichlorobenzene (ODCB) solution of Gd@C_{82}. Figure 1b show the UV-Vis-NIR spectra of Gd@C_{82}, TBPA, and their complexes with different molar ratios. It can be seen that the Gd@C_{82} exhibited characteristic absorbance at 403, 551, 638 and 724 nm, and TBPA showed strong absorbance at 382, 642 and 744 nm. When adding TBPA into Gd@C_{82} solution, absorption features of Gd@C_{82} weakened while the characteristic peaks of TBPA appeared (Figure 1b and Figure S5a), indicative of a electron (charge) transfer process from Gd@C_{82} to TBPA as conformed by mass spectrometry measurement (Figure S6).[33] It should be noted that after adding TBPA into Gd@C_{82} solution, a new peak at 522 nm emerged and its intensity increased with the addition of TBPA. Considering both the TBPA and Gd@C_{82} do not have obvious peak at 522 nm, thus this peak could be ascribed to the characteristic peak of Gd@C_{82}/TBPA complexes. Moreover, the intensity of peak at 522 nm reached a maximum with a Gd@C_{82}/TBPA ratio of 1: 8, which was confirmed by the Job's plot shown in Figure S5b, indicating that the most stable Gd@C_{82}/TBPA complex has a molar ratio of 1: 8, that is to say, one Gd@C_{82} molecule can be completely surrounded by eight TBPA molecules. For comparison, TBPA was added to C_{60} solutions but no obvious new peak was found, implying it is difficult to oxidize C_{60} by using TBPA (Figure S5c).

Stable Gd@C_{82}/TBPA complex was prepared by mixing the Gd@C_{82} and TBPA in ODCB solution thoroughly and then precipitating the complex in diethyl ether (for details please see ESI). Furthermore, inductively coupled plasma-atomic emission spectrometry (ICP-AES) and X-ray photoelectron spectrum (XPS) were performed to determine the composition of the as-prepared Gd@C_{82}/TBPA complex (Figure S9).[34] The results showed that the atomic ratio for Gd and Sb is nearly 1: 8, which is in good agreement with above UV-Vis-NIR result, indicating that one Gd@C_{82} molecule is surrounded by about eight TBPA molecules. Otherwise, XRD and TGA were carried out to characterize the complex, see Figure S10 and S11.

In addition, this oxidation could be executed in solid-liquid process, i.e. the aggregated Gd@C_{82} powder, which is almost impossible to re-dissolve, could be well resolved when adding TBPA in ODCB solution with the formation of Gd@C_{82}/TBPA complexes (see Figure S12). This method is very useful to recover the aggregated Gd@C_{82} solid.

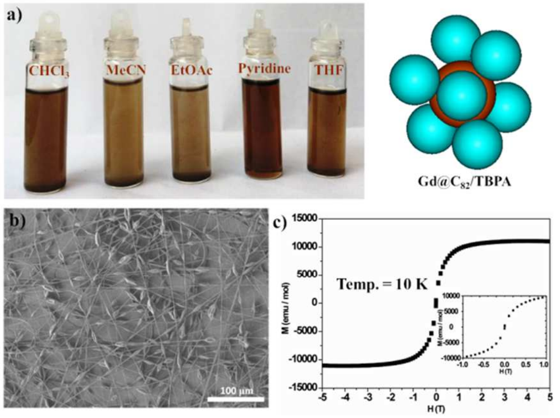

Figure 2. a) Optical images of solutions of Gd@C_{82}/TBPA in $CHCl_3$, MeCN, EtOAc, Pyridine, and THF (from left to right in sequences). b) SEM image of the Gd@C_{82}/TBPA-PVP complex film fabricated via electrospinning and c) its magnetization vs. field plot (inset: an enlarged M-H plot).

Table 1. The solubility (mg • mL^{-1}) of Gd@C_{82}/TBPA and Gd@C_{82} in several organic solvents.

	$CHCl_3$	MeCN	EtOAc	Pyridine	THF
Gd@C_{82}/TBPA	26.17	8.15	7.73	42.25	29.00
Gd@C_{82}	0.34	< 0.1	< 0.1	1.97	0.42

Unprecedentedly, formation of Gd@C_{82}/TBPA salt makes this new compound soluble in most common organic solvents such as chloroform ($CHCl_3$), acetonitrile (MeCN), ethyl acetate (EtOAc), pyridine, and tetrahydrofuran (THF) as shown in Figure 2a, whereas the pristine Gd@C_{82} has very low solubility in these solvents (Table 1 and Figure S13). Table 1 shows the solubility of Gd@C_{82}/TBPA in several organic solvents. Specifically, this new compound has solubility in EtOAc as large as 7.73 mg mL^{-1} where Gd@C_{82} could not dissolve. In addition, the Gd@C_{82}/TBPA could dissolve in $CHCl_3$ and THF with solubility of 26.17 and 29.00 mg mL^{-1} respectively, which greatly exceed those for pristine Gd@C_{82}. Such increased solubility of this new compound containing Gd@C_{82} would extend the potential application of Gd@C_{82} in many other research fields.

Moreover, the recycling of Gd@C_{82} from Gd@C_{82}/TBPA complex was studied subsequently. Briefly, the Gd@C_{82}/TBPA powder was put into deionized water and sonicated for 30 min, the suspended solid was treated by hydrochloric acid. The obtained solid was then extracted by ODCB and characterized by UV-Vis-NIR spectroscopy (Figure S14), which indicated that the Gd@C_{82}/TBPA has been decomposed and turned to Gd@C_{82}.

To expand the application of such highly soluble Gd@C_{82}/TBPA, a film of Gd@C_{82}/TBPA-PVP (polyvinylpyrrolidone) complex was successfully fabricated by electrospinning.[35-37] The morphology of the film can be tuned by changing the molecular weight and concentration of PVP (Figure S15). When the PVP with large molecular weight (ca. 1 300 000) was used in the electro-spinning process, microfibers dotted with knots were observed, see Figure 2b. Magnetization measurement performed on a superconducting quantum interference device (SQUID)[23-29] revealed that this Gd@C_{82}/TBPA-PVP film has super-paramagnetic property as shown in Figure 2c. This kind of paramagnetic fibers and film have potential applications in magnetic thin film materials.

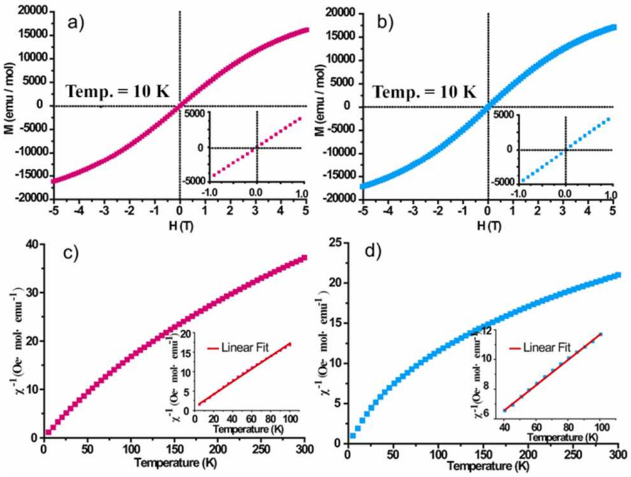

Figure 3. a, b) Magnetization vs. field plots (inset: an enlarged M-H plot) and c, d) magnetic susceptibility vs. temperature plots (inset: linear fit of the inverse susceptibility) of Gd@C_{82} (pink) and Gd@C_{82}/TBPA (blue) with molar ratio of 1: 8, respectively.

Figure 3 show the magnetic behaviors of Gd@C_{82} and Gd@C_{82}/TBPA powders. As can be seen from the magnetization (M) versus field (H) plots, both of them exhibited superparamagnetism at low temperature. For a paramagnetic system, the inverse magnetic susceptibility as a function of temperature is fitted to the Curie-Weiss law,[23-29]

$$\chi^{-1}(\mathrm{T}) = (\mathrm{T} - \theta)/\mathrm{C} \qquad (1)$$

where

$$\mathrm{C} = N\mu_{\mathrm{eff}}^2/3Ak \qquad (2)$$

where θ is Curie temperature, C is the Curie constant, N is the Avogadro's number, A is the atomic weight, and k is the Boltzmann constant. Utilizing a least squares method, we obtained the μ_{eff} of 7.00 μ_{B} for Gd@C_{82} with C = 6.13 K • emu • Oe^{-1} • mol^{-1} and θ = -5.40 K (T < 100 K), which is consistent with the previously reported values.[28,29] For Gd@C_{82}/TBPA, the calculated μ_{eff} is 9.68 μ_{B}, where C = 11.72 K • emu • Oe^{-1} • mol^{-1} and θ = -38.89 K (40 < T < 100 K). As expected, the μ_{eff} of Gd@C_{82}/TBPA was enhanced caused by the diminished antiferromagnetic coupling interaction of the unpaired spin on the C_{82} cage and the 4*f*-spin of the encapsulated Gd^{3+} ion. It is worth noting that Gd@C_{82}/TBPA exhibited slight antiferromagnetism below 40 K, which may be attributed to the crystallization of this complex, leading to an antiparallel arrangement of the electron spins.

To elucidate the spin coupling interaction, electron paramagnetic resonance (EPR) measurement was performed as shown in Figure S16. Although there is an unpaired electron spin delocalized on C_{82} cage, the half-filled 4*f* electronic shell of internal Gd^{3+} ion makes the EPR spectrum un-splitting,[38] and consequently, the Gd@C_{82} will show a broad EPR signal even at a relatively low temperature. The EPR spectrum of pristine Gd@C_{82} measured at 173 K has a main peak with g = 2.009 ascribed to the unpaired spin of C_{82}^{3+} cage as well as the 4*f*-electron spins of Gd^{3+}, and other small peaks at sides belong to the couplings between these two kinds of spin. When adding TBPA into Gd@C_{82} solution, the side-peaks faded away, indicative of the weakened spin-spin couplings caused by the lost electron spin on C_{82} cage. With increasing the amount of TBPA in the ODCB solution of Gd@C_{82}, the central peak became broader and weaker, revealing that the charge transfer between TBPA and the fullerene cage further quenched the unpaired spins on the C_{82}^{3+} cage.

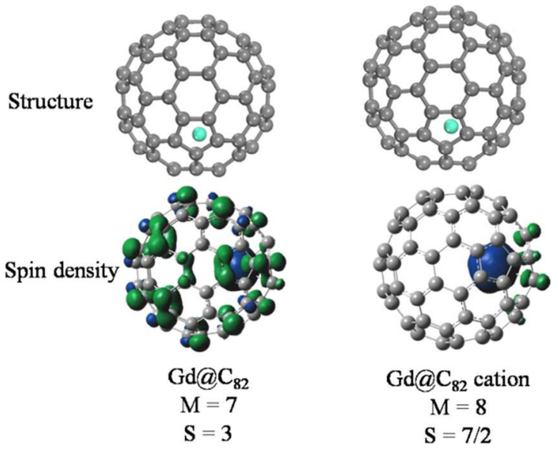

Figure 4. Calculated structures and spin density distributions of Gd@C_{82} and Gd@C_{82} cation.

In order to further disclose the magnetic property of Gd@C_{82}/TBPA, the structures of Gd@C_{82} and Gd@C_{82} cation were calculated, as shown in Figure 4. The results show that these two species have similar geometry except for the slight spatial displacement of Gd atom. The spin multiplicity (M) values of optimized Gd@C_{82} and Gd@C_{82} cation are 7 and 8, respectively.[10] According to the reported experiments in literatures, the spin quantum number (S) for Gd@C_{82} and Gd@C_{82} cation should be 3 and 7/2, respectively.[23-29] It can be seen that in Gd@C_{82}/TBPA, the Gd@C_{82} cation has improved spin characters and magnetic property.

In summary, we synthesized a kind of Gd@C_{82} salt, named Gd@C_{82}/TBPA, whose μ_{eff} is improved due to elimination of unpaired spin on C_{82} cage. The as-prepared Gd@C_{82}/TBPA can dissolve in many organic solvents and such high solubility will make it more applicable as magnetic material. The prepared paramagnetic fibers and film of Gd@C_{82}/TBPA-PVP complex will motivate the application of this new material.

This work was supported by the National Natural Science Foundation of China (21203205, 61227902, 51472248, 51472208), National Basic Research Program (2012CB932901), NSAF (11179006). T. Wang particularly thanks the Youth Innovation Promotion Association of CAS.

Notes and references

[a] *Beijing National Laboratory for Molecular Sciences, Laboratory of Molecular Nanostructure and Nanotechnology, Institute of Chemistry, Chinese Academy of Sciences, Beijing 100190, China. Tel: 86-10-82624962; E-mail: wangtais@iccas.ac.cn*

[b] *Key Laboratory of Interface Science and Engineering in Advanced Materials, Taiyuan University of Technology, Ministry of Education, Research Center of Advanced Materials Science and Technology, Taiyuan University of Technology, Taiyuan 030024, China*

† Electronic Supplementary Information (ESI) available: Experimental details, HPLC chromatogram, MALDI-TOF-MS profiles, XPS, TGA, XRD and EPR. See DOI: 10.1039/b000000x/

‡ *These authors contribute equally to this work.*

1 M. Yamada, T. Akasaka and S. Nagase, *Acc. Chem. Res.*, 2009, **43**, 92-102.

2 H. Yang, C. Lu, Z. Liu, H. Jin, Y. Che, M. M. Olmstead and A. L. Balch, *J. Am. Chem. Soc.*, 2008, **130**, 17296-17300.

3 Y.-J. Guo, T. Yang, S. Nagase and X. Zhao, *Inorg. Chem.*, 2014, **53**, 2012-2021.

4 C. M. Beavers, M. N. Chaur, M. M. Olmstead, L. Echegoyen and A. L. Balch, *J. Am. Chem. Soc.*, 2009, **131**, 11519-11524.

5 B. Q. Mercado, C. M. Beavers, M. M. Olmstead, M. N. Chaur, K. Walker, B. C. Holloway, L. Echegoyen and A. L. Balch, *J. Am. Chem. Soc.*, 2008, **130**, 7854-7855.

6 M. Krause and L. Dunsch, *Angew. Chem. Int. Ed.*, 2005, **44**, 1557-1560.

7 E. Nishibori, K. Iwata, M. Sakata, M. Takata, H. Tanaka and H. Kato, H. Shinohara, *Phys. Rev. B*, 2004, **69**, 113412.

8 T. Akasaka, T. Kono, Y. Takematsu, H. Nikawa, T. Nakahodo, T. Wakahara, M. O. Ishitsuka, T. Tsuchiya, Y. Maeda and M. T. Liu, *J. Am. Chem. Soc.*, 2008, **130**, 12840-12841.

9 L. Liu, B. Gao, W. Chu, D. Chen, T. Hu, C. Wang, L. Dunsch, A. Marcelli, Y. Luo and Z. Wu, *Chem. Commun.*, 2008, 474-476.

10 A. Sebetci and M. Richter, *J. Phys. Chem. C*, 2009, **114**, 15-19.

11 G.-P. Yan, L. Robinson and P. Hogg, *Radiography*, 2007, **13**, 5-19.

12 K. B. Ghiassi, M. M. Olmstead and A. L. Balch, *Dalton Trans.*, 2014, **43**, 7346-7358.

13 M. Shevtsov, B. Nikolaev, Y. Y. Marchenko, L. Yakovleva, A. Dobrodumov, G. Török, E. Pitkin and V. Lebedev, *Appl. Magn. Reson.*, 2014, **45**, 303-314.

14 C.-Y. Shu, L.-H.Gan, C.-R.Wang, X.-l.Pei and H.-b. Han, *Carbon*, 2006, **44**, 496-500.

15 J. Zhang, P. P. Fatouros, C. Shu, J. Reid, L. S. Owens, T. Cai, H. W. Gibson, G. L. Long, F. D. Corwin and Z.-J. Chen, *Bioconjugate Chem.*, 2010, **21**, 610-615.

16 J. Zhang, Y. Ye, Y. Chen, C. Pregot, T. Li, S. Balasubramaniam, D. B. Hobart, Y. Zhang, S. Wi and R. M. Davis, *J. Am. Chem. Soc.*, 2014, **136**, 2630-2636.

17 M. Mikawa, H. Kato, M. Okumura, M. Narazaki, Y. Kanazawa, N. Miwa and H. Shinohara, *Bioconjugate Chem.*, 2001, *12*, 510-514.

18 B. Sitharaman, R. D. Bolskar, I. Rusakova and L. J. Wilson, *Nano Lett.*, 2004, **4**, 2373-2378.

19 J.-J. Yin, F. Lao, P. P. Fu, W. G. Wamer, Y. Zhao, P. C. Wang, Y. Qiu, B. Sun, G. Xing and J. Dong, *Biomaterials*, 2009, **30**, 611-621.

20 T. Da Ros and M. Prato, *Chem. Commun.*, 1999, 663-669.

21 L. Bogani and W. Wernsdorfer, *Nat. Mater.*, 2008, **7**, 179-186.

22 M. Wolf, K. H. Müller, Y. Skourski, D. Eckert, P. Georgi, M. Krause and L. Dunsch, *Angew. Chem. Int. Ed.*, 2005, **44**, 3306-3309.

23 A. Svitova, Y. Krupskaya, N. Samoylova, R. Kraus, J. Geck, L. Dunsch and A. Popov, *Dalton Trans.*, 2014, **43**, 7387-7390.

24 A. Tiwari, G. Dantelle, K. Porfyrakis, A. A. Watt, A. Ardavan and G. A. D. Briggs, *Chem. Phys. Lett.*, 2008, **466**, 155-158.

25 H. Funasaka, K. Sugiyama, K. Yamamoto and T. Takahashi, *J. Phys. Chem.*, 1995, **99**, 1826-1830.

26 H. Huang, S. Yang and X. Zhang, *J. Phys. Chem. B*, 2000, **104**, 1473-1482.

27 H. Huang, S. Yang and X. Zhang, *J. Phys. Chem. B*, 1999, **103**, 5928-5932.

28 H. Funasaka, K. Sakurai, Y. Oda, K. Yamamoto and T. Takahashi, *Chem. Phys. Lett.*, 1995, **232**, 273-277.

29 U. Atzmony, M. Dariel, E. Bauminger, D. Lebenbaum, I. Nowik and S. Ofer, *Phys. Rev. B*, 1973, **7**, 4220.

30 A. Griesmaier, J. Werner, S. Hensler, J. Stuhler and T. Pfau, *Phys. Rev. Lett.*, 2005, **94**, 160401.

31 Y. Maeda, J. Miyashita, T. Hasegawa, T. Wakahara, T. Tsuchiya, L. Feng, Y. Lian, T. Akasaka, K. Kobayashi and S. Nagase, *J. Am. Chem. Soc.*, 2005, **127**, 2143-2146.

32 K. Furukawa, S. Okubo, H. Kato, H. Shinohara and T. Kato, *J. Phys. Chem. A*, 2003, **107**, 10933-10937.

33 K. Akiyama, T. Hamano, Y. Nakanishi, E. Takeuchi, S. Noda, Z. Wang, S. Kubuki and H. Shinohara, *J. Am. Chem. Soc.*, 2012, **134**, 9762.

34 J. Wu, N. Wang, Y. Zhao and L. Jiang, *J. Mater. Chem. A*, 2013, **1**, 7290-7305.

35 N. Wang, Y. Zhao, L. Jiang and *Macromol. Rapid. Comm.*, 2008, **29**, 485-489.

36 Q. Zhao, Z. Huang, C. Wang, Q. Zhao, H. Sun and D. Wang, *Mater. Lett.*, 2007, **61**, 2159-2163.

37 A. Sebetci and M. Richter, *J. Phys. Chem. C*, 2009, **114**, 15.

38 S. Hino, K. Umishita, K. Iwasaki, T. Miyazaki, T. Miyamae, K. Kikuchi and Y. Achiba, *Chem. Phys. Lett.*, 1997, **281**, 115-122.

Table of Contents

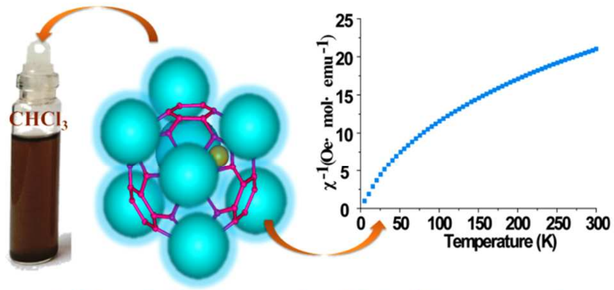

Highly soluble magnetic Gd@C$_{82}$/TBPA complex

A stable complex of highly soluble Gd@C$_{82}$/TBPA with improved paramagnetism and extended application was investigated.